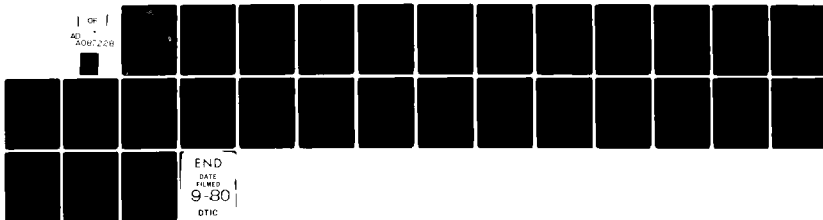


AD-A087 228

GEORGIA INST OF TECH ATLANTA CENTER FOR THE ADVANCEM--ETC F/G 20/11
NUMERICAL MODELING OF DYNAMIC CRACK PROPAGATION IN FINITE BODIE--ETC(U)
JUN 80 T NISHIOKA, S N ATLURI N00014-78-C-0636
6IT-CACH-SNA-25 NL

UNCLASSIFIED

1 OF 1
AD
A087228



END
DATE
FILMED
9-80
DTIC

ADA 087228

LEVEL II

①
P.S.

①⑤ Office of Naval Research
Contract ~~NO~~0014-78-C-0636 NR 064-610

⑨ Technical Report No. 9

Report No. GIT-CACM-SNA-25, *TR-11*

①④

⑥
NUMERICAL MODELING OF DYNAMIC CRACK PROPAGATION IN FINITE BODIES,
BY MOVING SINGULAR ELEMENTS, PART II. RESULTS,

by

Citya

①⑩ T. Nishioka ~~and~~ S.N./Atluri

DTIC
ELECTE
JUL 25 1980
S D C

①① JUN 80

12 29

Center for the Advancement of Computational Mechanics
School of Civil Engineering ✓
Georgia Institute of Technology
Atlanta, Georgia 30332

This document has been approved
for public release and sale; its
distribution is unlimited.

80 7 24 035
11 865

DDC FILE COPY

NUMERICAL MODELING OF DYNAMIC CRACK PROPAGATION IN FINITE BODIES,
BY MOVING SINGULAR ELEMENTS - PART II. RESULTS

T. Nishioka* and S. N. Atluri**
Center for the Advancement of Computational Mechanics
School of Civil Engineering
Georgia Institute of Technology, Atlanta, Georgia

Abstract

Using the moving-singularity finite element method described in Part I of this paper, several problems of dynamic crack propagation in finite bodies have been analysed. Discussions of the effects of wave interactions on the dynamic stress-intensity factors are presented. The obtained numerical results are compared with the corresponding infinite domain solutions and other available numerical solutions for finite domains.

Introduction

In Part I of the present paper [1], a "moving singular-element" procedure has been presented for the dynamic analyses of problems of fast crack propagation in arbitrarily shaped finite bodies with linear elastic material behaviour. In this procedure a singular-element, within which a large number of analytical eigen-functions corresponding to a propagating crack are used as basis functions for displacements, may be translated by an arbitrary amount $\Delta \Sigma$ in each time increment Δt of the numerical time-integration procedure. The moving singular-element, within which the crack-tip has always a fixed location, retains its shape at all times, while the mesh of "regular" (isoparametric) finite elements, surrounding the moving singular element, deforms accordingly. An energy-consistent variational statement was developed, as a basis for the above "moving singularity" finite-element method of dynamic crack propagation analysis. It

*Research Scientist

**Regents' Professor of Mechanical Engineering, Member ASME

has been shown [1] that the present procedure leads to a direct evaluation of the dynamic stress-intensity factors.

In the present Part II of the paper several numerical studies of stationary as well as propagating cracks in finite bodies, are presented. These studies, in general, fall into the category of linear elastic dynamic fracture mechanics. These studies, in addition to illustrating the efficiency and accuracy of the present procedure, also shed light on the effects of stress-wave interactions on the stress-intensity factors for dynamically propagating cracks in finite bodies.

The presently considered examples include: (i) static extension of a central crack in a panel from a non-zero initial length; (ii) self similar, constant-velocity, propagation from a finite initial length of a central crack in a finite plane body subject to an uniform, time-independent, tensile stresses (normal to crack-axis) at the edges (which problem, is analogous to that treated by Broberg [2], and Rose [3,4]); (iii) a stationary central crack in a finite plane body subject, at its edges, to a Mode I type uniformly distributed stress with a Heaviside step-function time-dependence (analogous to the problems of Baker [5], Sih, Embley and Ravera [6], and Thau and Lu [7]); (iv) a problem similar to that in (iii) except that the crack-tips remain stationary until a time t_0 , where upon they start propagating at a constant speed (analogous to the problems studied by Freund [8]); and (v) constant-velocity propagation of an edge-crack in a panel, with the direction of propagation being parallel to the panel-edges on which uniform displacements, normal to the edges, are prescribed (analogous to the problem treated by Nilsson [9]). All the references [2-8] deal with unbounded bodies, except [9] which deals with a finite height, but infinite width strip. Thus the presently obtained results for finite bodies are compared with those in [2-9]

and the effects of finiteness of the domains are discussed. Comparisons of the present results with the numerical results of other investigators, where available, are also presented and discussed.

In the following we present results for each of the problems cited above.

(i) Static Crack Extension

To test the accuracy of the present method of "moving singular-elements", first a static problem of a central-cracked square panel [$2L(\text{length}) = 2W(\text{width})$], subjected to uniform tension at edges parallel to the crack axis, was solved to obtain the static stress-intensity factor as a function of the current crack length, Σ . Thus, in the finite element development given in Part I of this paper [1], velocity and acceleration effects were ignored. The eigen-functions embedded in the singular-element reduce, when $v = 0$, to the well-known Williams' eigen-functions as shown in Appendix A of [1]. Starting from an initial crack length value of $\Sigma_0 = 0.2W$, the singularity element was successively translated (in Mode I growth sense), statically (with $v = 0$) in increments of $\Delta\Sigma = 0.005W$ until a final value of crack length $\Sigma = 0.5W$ is reached. During the above series of calculations, the externally applied uniform tension was held constant. At each current crack-length level, the stress-intensity factor is computed directly as an unknown from the finite element equations, as described in [1]. From the normalized stress-intensity factor solutions shown in Fig. 1, it is seen that the present results agree excellently with those reported by Isida [10]. The normalized results shown in Fig. 1 may be viewed as correction factors for static stress-intensities, due to the finite size of the panel.

We note that the symbols (t) in Fig. 1, as well as in all the subsequent Figures, denote the current crack length (Σ/W) where the regular elements surrounding the moving crack-element were readjusted as described in Fig. 2 of [1].

(ii) Self-Similar, Constant Velocity, Crack-Propagation from a Finite Initial Length

The problem is that of a centrally cracked square panel ($L = W = 40\text{mm}$) with properties: μ (shear modulus) = $2.94 \times 10^{10} \text{ N/mm}^2$; ν (Poisson's ratio) = 0.286; ρ (Mass density) = $2.45 \times 10^3 \text{ Kg/m}^3$. A time-independent tensile stress was assumed to be acting at the edges of the specimen parallel to the crack-axis. The crack is assumed to open from an initial length $(\Sigma_0/W) = 0.2$ and to grow symmetrically with a constant velocity, v . This problem may be considered to be similar to that treated by Broberg [2] except that Broberg treated an infinite body with a crack which opens from a zero initial length. The problem was analyzed for four different values of v , namely, $(v/C_s) = 0.2, 0.4, 0.6$ and 0.8 respectively, where the shear wave speed for the present problem is $C_s = 3.4641 \times 10^6 \text{ mm/sec}$. The dilatational and surface (Rayleigh) wave speeds, C_d and C_R , respectively, are such that: $(C_d/C_s) = 1.8266$, and $(C_R/C_s) = 0.9238$.

In all the four considered cases of (v/C_s) ratio, the increment of crack growth in each step, $\Delta\Sigma$, was kept the same, at the value: $(\Delta\Sigma/W) = 0.005$. Thus, in each of the considered (v/C_s) cases, the time integration step, Δt , changes according as: $[(v \cdot \Delta t)/\Sigma] = 0.005$. The finite element mesh used, at the initial crack length in each of the four cases, is shown in the inset of Fig. 3. In this Figure, as well as in Figs. (1, 6 and 9), the singular-element near the crack-tip is identified by hatched markings.

As noted in the review article by Rose [3], the dynamic stress intensity factor K may be expressed as the product of a velocity factor $k(v)$ and a static factor K^* ; thus,

$$K = k(v) K^* \quad (1)$$

The "static factor" K^* depends on the current length of the crack, the applied load, the history of crack extension, but not on the instantaneous crack speed.

As also discussed in [3], K^* is, in general, not equal to the static stress-intensity factor, K_S , for a stationary crack of the same length as the moving crack. The analytical expression for $K^{*\infty}$ (in an infinite body subjected to uniform stress normal to the crack axis), as a function of the current crack length is given by Eshelby [11] and in [3], as:

$$K^{*\infty} = (2/\pi)^{1/2} \int_{\Sigma_0}^{\Sigma} \sigma_{yy}(x)/(\Sigma - x)^{1/2} dx \quad (2)$$

$$\text{where, } \sigma_{yy}(x) = \sigma |x|/(x^2 - \Sigma_0^2)^{1/2} \quad ; \quad |x| > \Sigma_0 \quad (3)$$

In Eqs. (2 and 3), σ is the applied tensile stress at infinity, $2\Sigma_0$ is the initial crack length, and x, y are cartesian coordinates centered such that $x = \pm \Sigma(t)$ denote the current crack-tips and y is normal to crack-axis. Thus $\sigma_{yy}(x)$ in Eq. (2) is the initial distribution of stress along the axis of the crack, prior to its' propagation. Eshelby's results for the integral in Eq. (2) is:

$$K^{*\infty} = [\sigma(\pi\Sigma_0)^{1/2} (2/\pi) \{(2+\xi) E-F\}]/[1+(\xi/2)]^{1/2} \quad (4)$$

where $\xi = (\Sigma - \Sigma_0)/\Sigma_0$; and E and F are the complete elliptic integrals of the 2nd and 1st kind, respectively, with the modulus $[\xi/(2+\xi)]^{1/2}$. On the other hand, the static-stress intensity factor K_S^∞ for a crack of length 2Σ in an infinite domain is,

$$K_S^\infty = \sigma(\pi\Sigma)^{1/2} \quad (5)$$

Thus, in general, $K^{*\infty} < K_S^\infty$. It is also noted that the Eq. (4) for $K^{*\infty}$ is valid only until the time that disturbances from one crack-tip reach the other (moving) crack-tip. However, for the case of a crack growing self-similarly from a zero initial length ($\Sigma_0 = 0$) with a constant velocity v , as in the problem studied by Broberg [2], disturbances from one crack tip influence at all times the other moving crack tip if $2v < c_d$, and $K^{*\infty} \equiv K_S^\infty$ at all times.

The normalized dynamic stress-intensity factor solution for the present problem of a crack, in a finite square panel, propagating self-similarly at a constant velocity $(v/C_s) = 0.2$, is shown in Fig. 2. Note that the normalization is such that a value of unity represents the normalized stress intensity factor K_s^∞ for a crack of length $2\Sigma(\Sigma = \Sigma_0 + vt)$ in an infinite solid with time-independent remote tension σ . Also shown in Fig. (2) are: (i) the finite-size correction factor $F = K_s^f / \sigma(\pi\Sigma)^{1/2}$ for the static stress-intensity factor K_s^f in the present finite domain; (ii) the normalized "static" factor $K^{*\infty} / \sigma(\pi\Sigma)^{1/2}$, as calculated from Eq. (4), and (iii) the velocity factor $k(v)$ for $(v/C_s) = 0.2$, as given by Broberg [2]. The effect of the finiteness of the domain on K^* may be accounted for, approximately, by including a finite-size correction factor in the initial stress-distribution at Σ_0 , in Eq. (3) above. Thus it appears that one may write, approximately, that $K^{*f} = F(\Sigma_0)K^{*\infty}$. For the present case of $(\Sigma_0/W) = 0.2$, the finite correction factor $F(\Sigma_0) \approx 1.055$, as seen from Fig. 1.

Also marked in Fig. 2 are several specific instants of time (or equivalently), the corresponding values of Σ with the notations: (a) D_c , S_c and R_c are, respectively, the times taken by the dilatational, shear and Rayleigh waves to traverse one crack-width, (b) $D_c D_c$ (or $R_c R_c$) denotes D_c (or R_c) plus the time for the first rescattered dilatational (or Rayleigh) waves to travel one crack-width; (c) $D_c D_f$ (or $S_c S_f$) denotes the time taken for the dilatational (or shear) waves emanated by one crack-tip to be reflected by the nearest free-boundary and reinteract with the crack-tip in question. The above times are calculated from the continuum relations for the respective wave speeds. However, it should be borne in mind that a "consistent-mass" representation is used in the present finite element method.

For the case of $(v/C_s) = 0.2$, it is seen from Fig. 2 that the computed normalized dynamic stress-intensity factor correlates excellently with the values given by $F(\Sigma_0)K^{*\infty}k(v)/\sigma(\pi\Sigma)^{1/2}$ until roughly the time denoted by R_c . At longer times, i.e., at the times greater than R_c and $D_c D_f$, the computed normalized dynamic $K_I(t)$ appears to correlate excellently with the values given by $\left[\beta K_S^f k(v) / \sigma(\pi\Sigma)^{1/2} \right]$ where β is a constant. It is interesting to observe that, for the present problem, this constant β appears to be equal to $G(\Sigma_{RC})/F(\Sigma_{RC})$ where $F(\Sigma_{RC})$ is the finite correction factor in the static stress-intensity for a crack of length equal to the current length, Σ_{RC} , in a dynamic problem, at which the event R_c (as defined earlier), occurs; whereas, $G(\Sigma_{RC})$ is likewise, the ratio $[F(\Sigma_0)K^{*\infty}/\sigma\sqrt{\pi\Sigma}]$ at $\Sigma = \Sigma_{RC}$. The event R_c is seen to occur at the time, $\tilde{t} = (2\Sigma_0)/(C_R - v)$, and thus, $\Sigma_{RC} = -\Sigma_0 + v\tilde{t}$. Both \tilde{t} and (Σ_{RC}/W) decrease as Σ_0 decreases, for given C_R and v . Thus, for smaller values of Σ_0 (and/or smaller values of v), the ratios $F(\Sigma_{RC})$, $G(\Sigma_{RC})$, and hence β tend to a value of unity. Thus, for cracks propagating from initial lengths such that $(\Sigma_0/W) \ll 1$, it appears that at the times greater than R_c and $D_c D_f$ and/or after the crack has grown dynamically to a few times its' initial length, the static factor K^{*f} approaches the static-stress-intensity factor for the current crack length in the finite body, namely, K_S^f .

In connection with the presently computed results shown in Fig. 2, it should be noted that the crack velocity, v , was taken to be zero at the initial crack length Σ_0 . It is assumed that the crack-tip accelerates to a velocity, $(v/C_s) = 0.2$, during the first time increment, Δt . The convergence of the present numerical results to the analytically predicted ones, at small times, $t \ll D_c$ in the present case of $(v/C_s) = 0.2$, could have been studied by altering this time step Δt in which the crack-tip accelerates from $(v/C_s) = 0$ to $(v/C_s) = 0.2$. However, this was not attempted.

The computed normalized dynamic stress-intensity factor solution for the case $(v/C_s) = 0.4$ is shown in Fig. 3, wherein the times D_c , S_c , $D_c D_f$ and R_c , as defined earlier, are also marked. Once again, it is seen that until significant interaction of the waves from the other crack-tip and the free surface takes place (ie., for time $t < R_c$ or $D_c D_f$), the computed dynamic K-factor for the finite body correlates excellently with the value predicted by the approximate function: $[K^{*f}_k(v)]$.

Finally, the results for the cases $(v/C_s) = 0.6$ and 0.8 , respectively, are shown in Fig. 4, wherein only the times D_c , and $D_c D_f$ are also marked. The values of R_c and S_c are greater than the time for which the solution is obtained. Once again, it is seen that the computed dynamic K-factor correlates well with the approximate prediction, $K^{*f}_k(v)$. However, the convergence of the computed solution, to that analytically predicted, is slow, at these higher crack-speeds. A possible reason for this may be the initial conditions at Σ_0 used in the present study, as explained earlier.

The crack-mouth opening displacements at various instants of time (or equivalently, at corresponding crack-lengths), for the case of $(v/C_s) = 0.4$, are shown in Fig. 5. Also shown in Fig. 5 are the corresponding analytical results by Broberg [2], who considers constant velocity crack-propagation starting from a zero initial crack-length. An excellent correlation between the present results and those of [2] is noted. A similar correlation was also noted for the other considered cases of (v/C_s) ratio, but are not shown here.

(iii) Stress-Wave Loading of a Stationary Crack in a Finite Body

The problem is that of a rectangular panel $[(w/L) = 2.6]$ with a centrally located crack of length $(\Sigma_0/W) = (3/13)$. The material properties are taken to be: μ (shear modulus) = 2.94×10^{10} N/mm²; $\nu = 0.286$; and $\rho = 2.45 \times 10^3$

kg/m³. Uniformly distributed uniaxial tensile stresses, with a Heaviside step-function time-dependence, were assumed to act at the edges of the panel parallel to the crack-axis. The crack is assumed to be stationary under the action of this time-dependent loading.

Due to symmetry, only a quadrant of the panel is modeled by finite elements, as shown in Fig. 6. Also marked in Fig. 6 are specific instants of time, calculated by using continuum wave speeds, with the notations: (a) D_m is the time taken by the dilatational waves to travel the distance from the boundary, where time-dependent tractions are applied, to the crack-tip; (b) $D_m D_c$, $D_m S_c$ and $D_m R_c$ are, respectively, equal to D_m plus the time taken by the first scattered dilatational, shear, and Raleigh waves to reach from one crack-tip to the other; (c) $D_m D_c D_c$ is equal to $D_m D_c$ plus the time taken by the first rescattered dilatational wave to travel one crack-width; (d) $D_m D_c D_f$ is equal to D_m plus the time taken by the scattered longitudinal waves to travel from the crack-tip to the nearest free boundary surface and back to the same crack-tip; (e) $D_m D_{ni}$ is the time taken by the dilatational waves to travel the length of the bar, reflect from the boundary surface on the opposite and return back to the crack-tip; and (f) $D_m D_m D_c$, $D_m D_m S_c$ and $D_m D_m R_c$ are, respectively, equal to $D_m D_m$ plus the time for the rescattered dilatational, shear and surface waves to travel one crack-width.

The presently computed normalized dynamic stress-intensity factor solution is shown in Fig. 6. Also shown in Fig. 6 are the analytical solutions by Baker [5], Sih, Embley and Ravera [6], for infinite domains, and the numerical solution by Aoki et al [12] for a finite domain identical to the one considered here. During the time interval D_m to $D_m D_c$, when no wave interaction takes place, the results for the present problem must agree with the results of Baker [5] and this can be seen to be the case with the present results. The solution at longer times is found to be in good agreement with that of Sih et al

[6]. It is noted that the overshoot in the k -factor at the time instant $D_m R_c$ in the present solution, as compared to the solution by Sih et al [6], is analogous to that in a recent solution by Kim [13]. It is also seen from Fig. 6, that the present solution is higher than that of Aoki et al [12] at all times. However, the solution by Aoki et al appears to be lower than that by Baker [5] even for times less than $D_m D_c$.

Finally, it is of interest to note that even though the time for the longitudinal wave to arrive from the loaded boundary to the crack, as computed from continuum wave speeds, is D_m as marked in Fig. 6, a nonzero stress-intensity is observed at the crack-tip even at times lower than D_m in the finite element solution. This is due to the inertia-coupling that exists between the finite element nodes (especially those of the singular-element) when a consistent mass-matrix, as in the present, is used.

(iv) Crack-Propagation at Constant Speed: Stress-Wave Loading

We consider the problem wherein the geometry, material properties and the time-dependent loading are all identical to those described under the case (iii) above. In this problem, the crack with an initial length of $(\Sigma_0/W) = 3/13$ remains stationary until a time $t_0 = 4.4 \mu s$ and then propagates with a constant velocity $v = 1000 \text{ m/sec}$. The finite element breakdown at the initial crack length, Σ_0 , is identical to that in Fig. 6. In modeling the crack propagation, the regular elements are periodically readjusted as indicated in Fig. 2 of [1]. The instants of time (or equivalently the value of \bar{z}) at which this readjustments are done, are marked, by (\dagger) in Fig. 7.

Also marked in Fig. 7 are several specific instants of time, calculated by using continuum wave speeds, with the notations: (a) D_m is the time for the dilatational waves to travel from the boundary, where a Heaviside step function tension is applied, to the stationary crack-tip. (b) $D_m D_c$, $D_m S_c$

and $D_m R_c$ are, respectively, equal to D_m plus the time taken by the dilatational, shear and surface waves first scattered by the stationary crack-tip to reach the other crack-tip; (c) D_c , S_c , R_c are, respectively, equal to t_0 (when the crack-tips begin to propagate) plus the time taken by the dilatational, shear and surface waves emanated by crack-tip at t_0 to reach the other crack-tip; (d) $D_m D_m$ is the time taken by the longitudinal waves to travel the length of the panel to the opposite side and return to a (moving) crack-tip; (e) $D_c D_m$ is the time taken for the dilatational waves emanating from a crack-tip at t_0 travel to the nearest boundary (which in this case is the one where tractions are applied) and back to the same crack-tip, (f) $D_m D_c D_f$ is equal to D_m plus the time taken by the dilatational waves first scattered by the stationary crack-tip to travel to the nearest free-boundary and back to the same crack-tip, which is now propagating; (g) $D_c D_f$ is equal to t_0 plus the time taken by the dilatational waves emanating from the crack-tip at t_0 to travel to the nearest free boundary and back to the same crack-tip.

The presently computed results for the dependence of the dynamic stress intensity factor on time are indicated in Fig. 7, along with the comparison (analytical) results by Freund [8] and Baker [5], and the (numerical) results by Aoki, et al [12]. As noted earlier, the correlation of the present stationary crack results with those of Baker [5], until wave interaction takes place, is excellent. In the case when the crack propagates suddenly at the time t_0 ($= 4.4 \mu s$ in Fig. 7), the infinite domain results by Freund [8] are seen to correlate excellently with the present results, until significant interaction of waves emanating from one crack-tip with the other crack-tip takes place. It is noted that in [8] the crack-tip velocity is assumed to change from zero to "v" in zero time, whereas, in the present numerical study, this transition is assumed to take place over a finite time-step Δt . For a closer comparison

with the results of [8], it would be interesting to vary the size of Δt over which the above transition occurs; but this is not pursued in the present study. It is seen that the comparison results by Aoki et al [12] are somewhat lower than those in [8] even until the time that the solution in [8] may be considered valid. Further, the results in [12] are higher than the present, after this time.

The crack-face opening displacements at various time intervals for the propagating crack, as well as similar results at corresponding times for a stationary crack are shown in Fig. 8. It is interesting to note that at sufficient distances away from the propagating crack-tip, the crack-mouth opening displacements are nearly the same for the stationary as well as propagating cracks.

(v) Constant Velocity Crack-Propagation in a Strip with Prescribed Boundary-Displacements

The problem considered is that of the constant velocity propagation of an edge crack in a square sheet whose edges parallel to the direction of crack-propagation are subject to uniform displacements \bar{u}_2 in the direction normal to that of crack-propagation. This problem is analogous to that treated by Nilsson [9] who obtained an analytical solution for the steady-state stress-intensity factor for the constant velocity propagation of a semi-infinite crack in a finite-height (normal to crack-axis), infinite-width, strip.

In the present problem the following geometry and material parameters are used: $(2h/W) = 1.0$ (see inset of Fig. 9), $\nu = 0.286$; $\mu = 2.94 \times 10^{10}$ N/mm², and $\rho = 2.45 \times 10^3$ Kg/m³. The crack is assumed to start to propagate from an initial length of $(z_0/h) = 0.4$.

Three different cases of constant velocity propagation, $(v/C_s) = 0.2$; 0.40, and 0.60, respectively, are considered.

The results for the dynamic stress-intensity factor for the case $(v/C_s) = 0.2$ are shown in Fig. 9 along with the analytical solutions by Nilsson [9]. The results in Fig. 9 are normalized with respect to the plane-strain, static ($v = 0$) stress intensity factor for the semi-infinite crack in a finite-height, infinite-width strip, namely, $K_S^\infty = \bar{u}_2 E / h^{1/2} (1 - \nu^2)$. Also shown in Fig. 9 are certain specific instants of time, with the notations: (a) $D_c D_{f1}$, $S_c S_{f1}$, are, respectively, the times taken by the dilational, and shear waves, emanated by the moving crack-tip to be reflected from the nearest free-boundary and travel back to the crack-tip; (b) $D_c D_{f2}$ is the time taken by the dilatational waves emanated from the crack-tip to be reflected by the second free-boundary ($x = W$) and travel back to the crack-tip.

It is seen from Fig. 9 that, the correlation between the present and Nilsson's [9] results is excellent. It may be of interest to note that in an analysis using the "node-release" technique, Malluck and King [14] found, for the case of $(v/C_s) = 0.325$, that their computed results for the energy-release rate for a similar problem were about 20% lower than that predicted by Nilsson [9], as steady-state conditions are reached. This may indicate the relative efficiency of the present numerical method as compared to the familiar "node-release" techniques.

Finally the computed results for the cases $(v/C_s) = 0.4$ and 0.6 are shown in Figs. 10 and 11 respectively. The times noted in Figs. 10 and 11 have the same meanings on those indicated in Fig. 9. From Figs. 10 and 11 it is once again seen that the present results agree excellently with those in [9].

Closure

The procedure of a "moving singular element", within which a large number of eigenfunctions for a propagating crack are embedded, has been applied to study several problems of dynamic crack propagation in finite

bodies. The numerical results have been found to correlate well with the available analytical solutions, for corresponding problems in infinite domains, during the time for which these analytical solutions may be considered as valid. The computed solutions beyond these times, and the knowledge of the times involved for wave-interaction in finite bodies, indicate both qualitatively and quantitatively the effects of stress-wave interactions on dynamic stress-intensity factors for cracks propagating in finite bodies.

The use of the presented numerical procedure in the simulation of experimental data from dynamic fracture test specimens, as well as in predicting crack-propagation history in dynamically loaded cracked bodies, are the subjects of a forthcoming paper.

Acknowledgements

This work was supported by the Office of Naval Research under Contract No. N0004-78-0636 with the Georgia Institute of Technology. The authors thank Dr. N. Perrone for his encouragement. Thanks are also expressed to Mrs. T. Rapp for her able typing of this manuscript.

References

1. Nishioka, T. and Atluri, S. N., "Numerical Modeling of Dynamic Crack Propagation in Finite Bodies, by Moving Singular Elements - Part I - Formulation" submitted herewith.
2. Broberg, K. B., "The Propagation of a Brittle Crack" Arkiv För Fysik, Band 18, No. 10, 1960, pp. 159-192.
3. Rose, L. R. F., "Review Article, Recent Theoretical and Experimental Results on Fast Brittle Fracture" International Journal of Fracture, Vol. 12, No. 6, 1976, pp. 799-813.
4. Rose, L. R. F., "On the Initial Motion of a Griffith Crack" International Journal of Fracture, Vol. 12, No. 6, 1976, pp. 829-841.
5. Baker, B. R., "Dynamic Stresses Created by a Moving Crack" Journal of Applied Mechanics, Trans. ASME, Vol. 29, 1962, pp. 449-545.
6. Sih, G. C., Embley, G. T. and Ravera, R. S., "Impact Response of a Finite Crack in Plane Extension" International Journal of Solids and Structures, Vol. 8, 1972, pp. 977-993.
7. Thau, S. A. and Lu, T.-H., "Transient Stress Intensity Factors for Finite Crack in an Elastic Solid Caused by a Dilatational Wave" International Journal of Solids and Structures, Vol. 7, 1971, pp. 731- .
8. Freund, L. B., "Crack-Propagation in an Elastic Solid Subjected to General Loading - III. Stress Wave Loading" Journal of Mechanics and Phys. Solids, Vol. 21, 1973, pp. 47-61.
9. Nilsson, F., "Dynamic Stress-Intensity Factors for Finite Strip Problems" International Journal of Fracture, Vol. 8, No. 4, 1972, pp. 403-411.
10. Isida, M., "Effect of Width and Length on Stress Intensity Factors of Internally Cracked Plates Under Various Boundary Conditions" International Journal of Fracture, Vol. 7, No. 3, 1971, pp. 301-306.
11. Eshelby, J. D., "The Elastic Field of a Crack Extending Non-Uniformly Under General Anti-plane Loading" Journal of Mechanics Phys. Solids, Vol. 17, 1969, pp. 177-199.
12. Aoki, S., Kishimoto, K., Kondo, H. and Sakata, M., "Elastodynamic Analysis of Crack by Finite Element Method Using Singular Element" International Journal of Fracture, Vol. 14, No. 11, 1978, pp. 59-68.
13. Kim, K. S., "Dynamic Propagation of a Finite Crack" International Journal of Solids and Structures, Vol. 15, 1979, pp. 685-699.
14. Malluck, J. F. and King, W. W., "Fast Fracture Simulated By a Finite-Element Analysis Which Accounts for Crack-tip Energy Dissipation" in Numerical Methods in Fracture Mechanics (Eds. Luxmore and Owen) University College, Swansea, 1978, pp. 648-659.

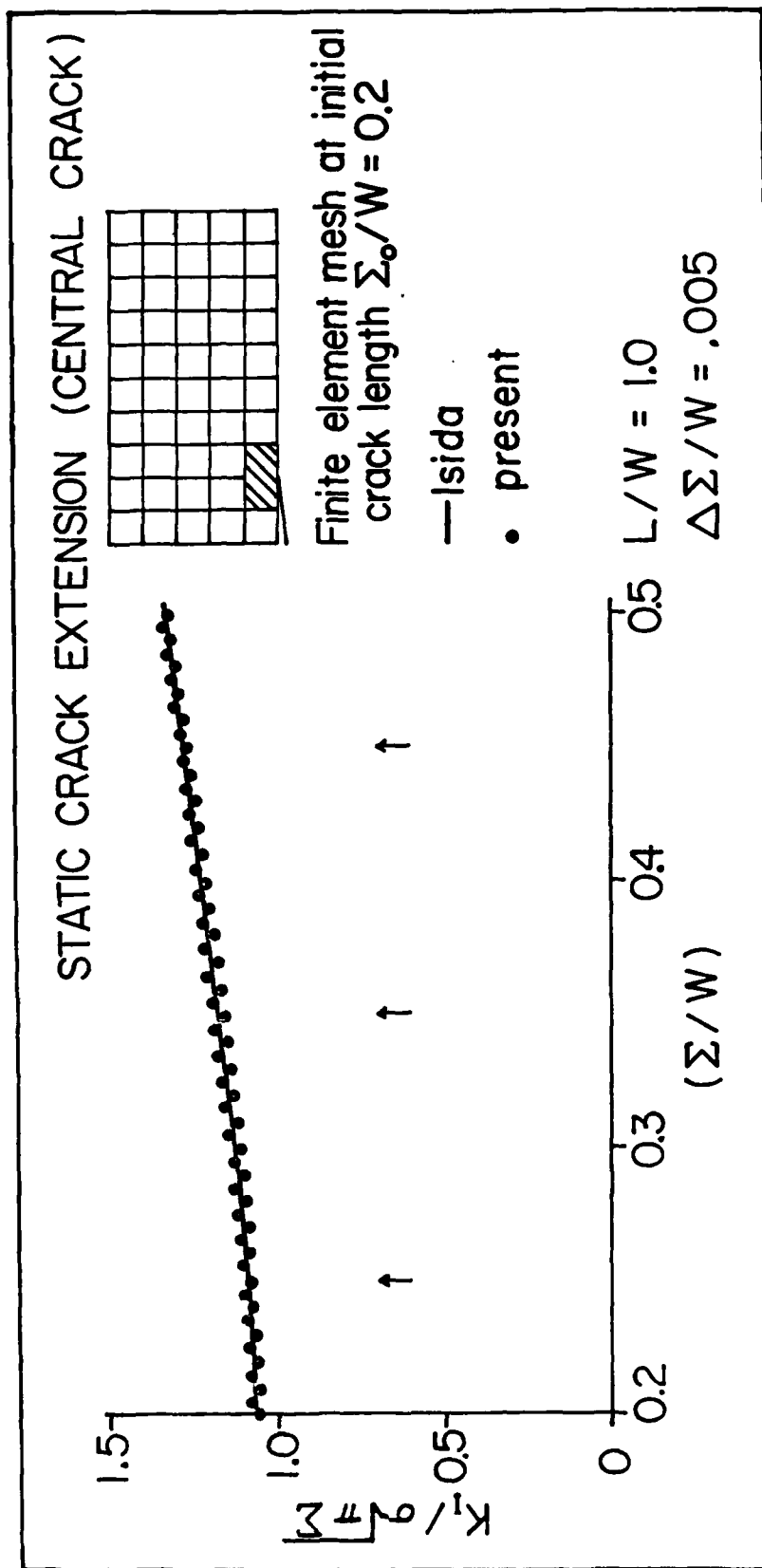


Fig. 1

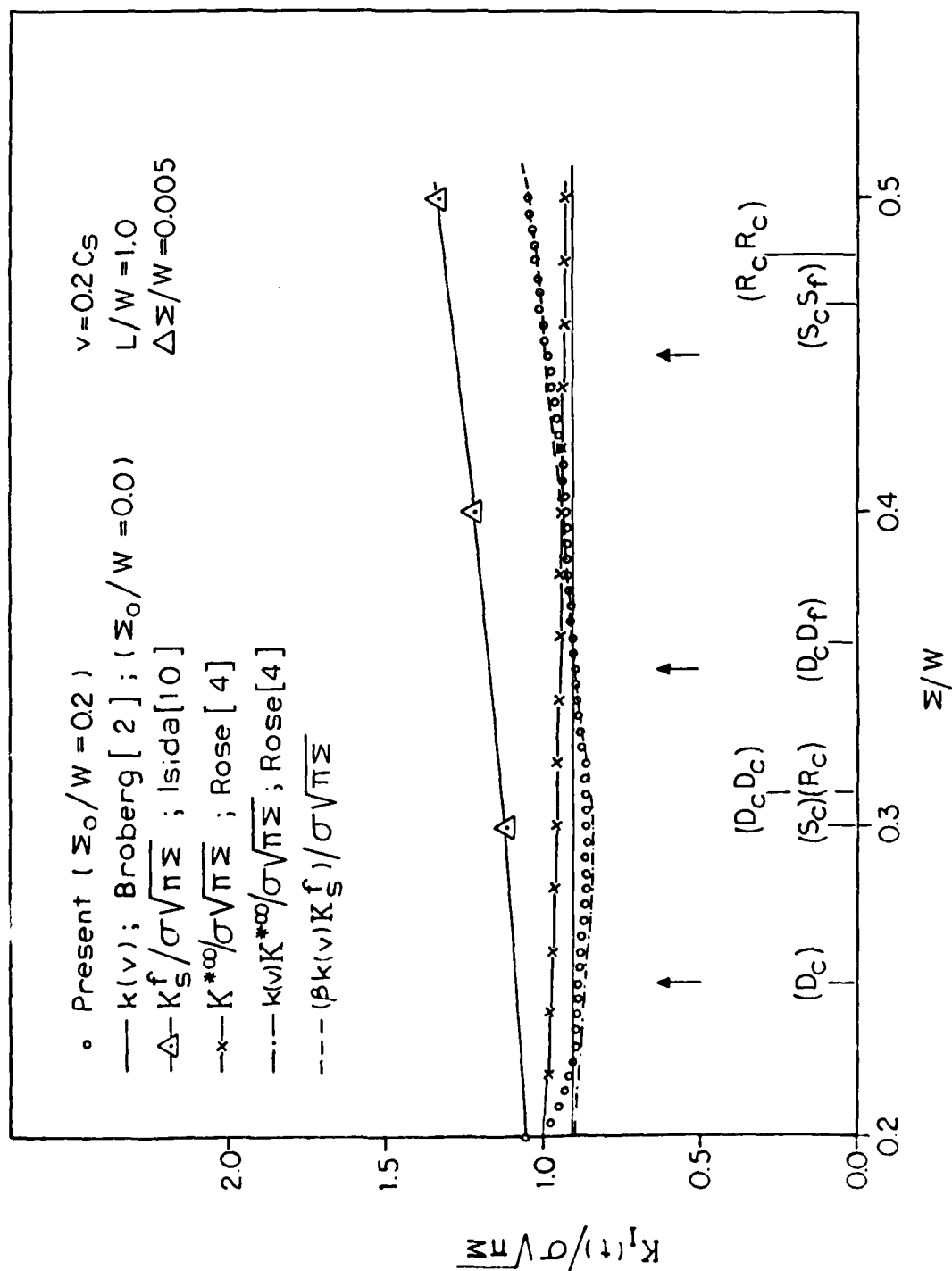
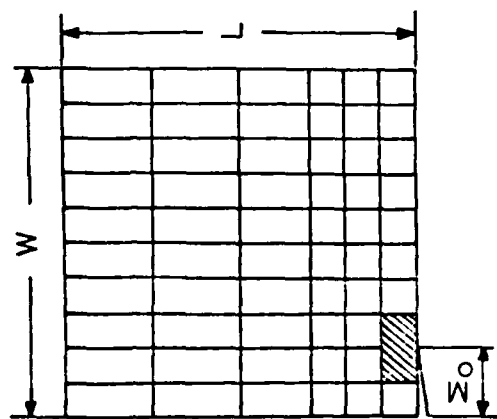


Fig. 2



$\nu = 0.4 C_S$
 $L/W = 1.0$
 $(\Delta \Sigma / W) = 0.005$

\circ Present $(\Sigma_0/W) = 0.2$
 $—$ $k(\nu)$; Broberg [2]; $(\Sigma_0/W) = 0.0$
 $---$ $k(\nu) K^* \omega / \sigma \sqrt{\pi \Sigma}$; Rose [4]

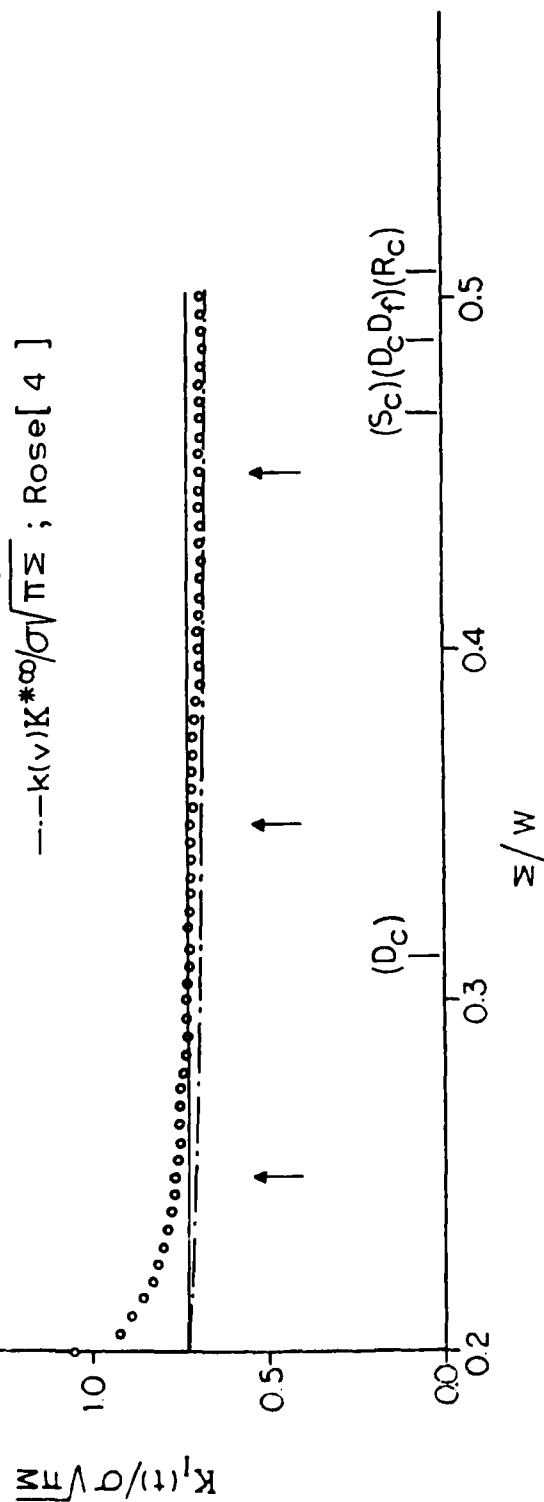
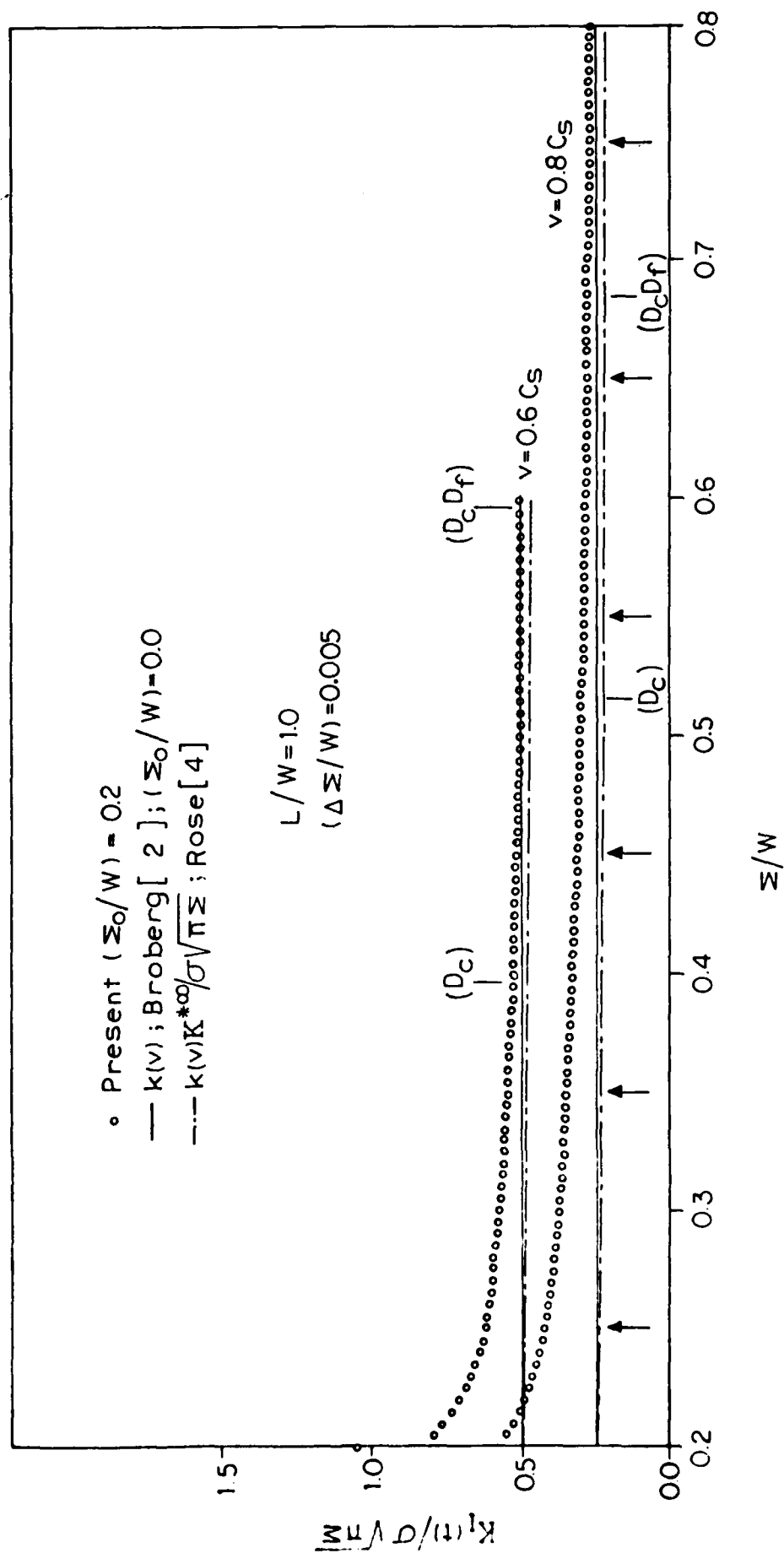


Fig. 3



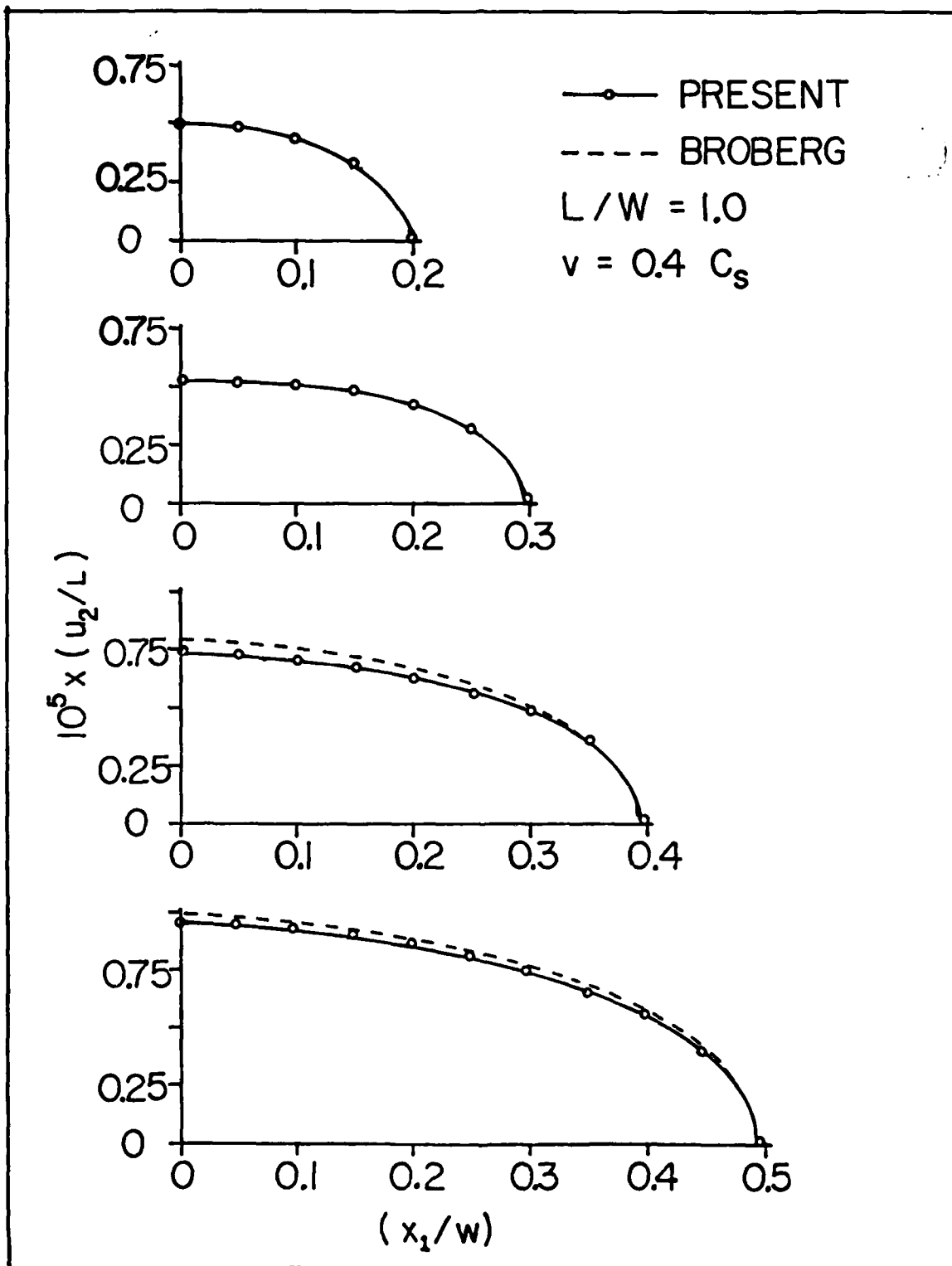


Fig. 5

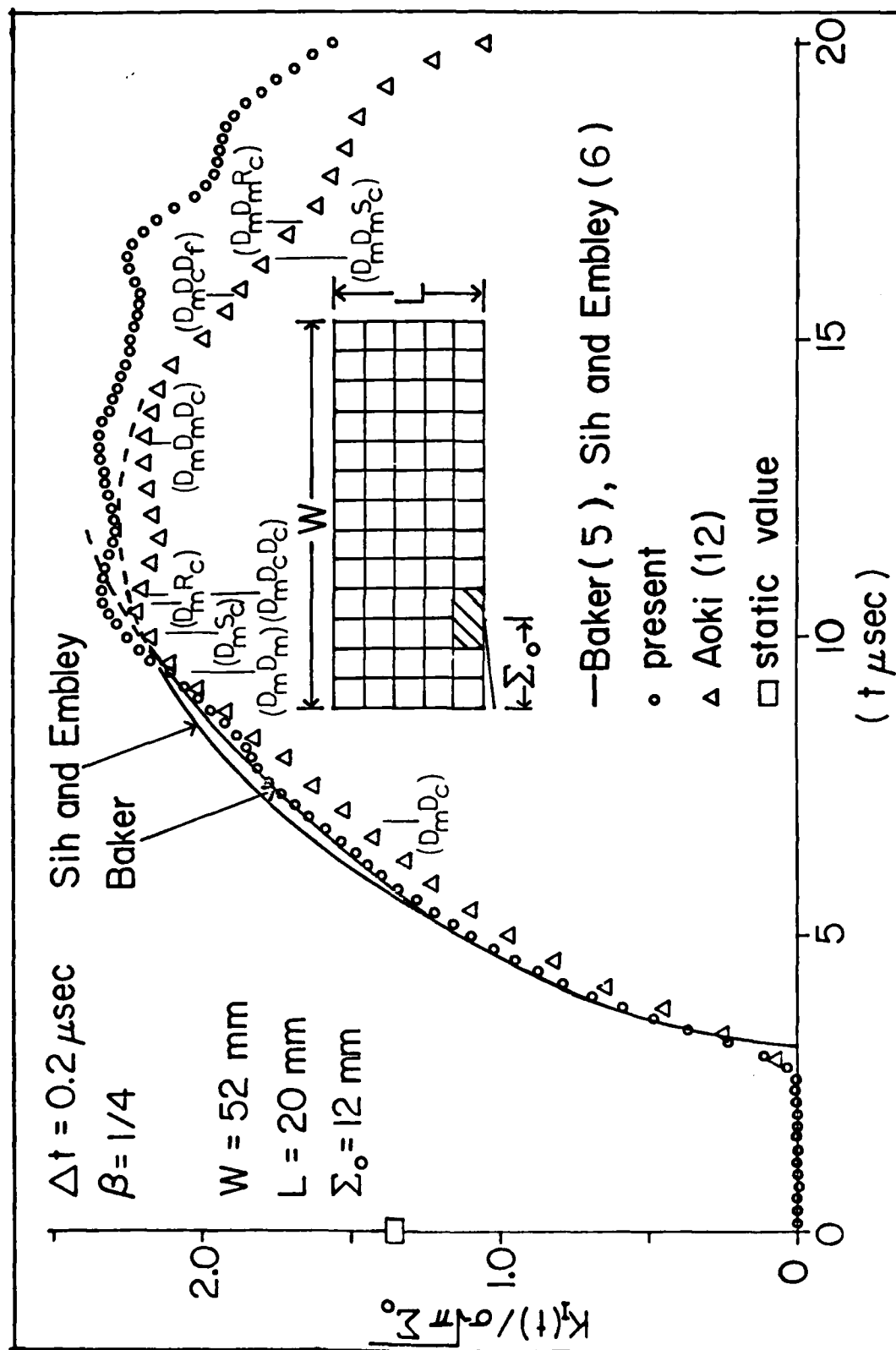


Fig. 6

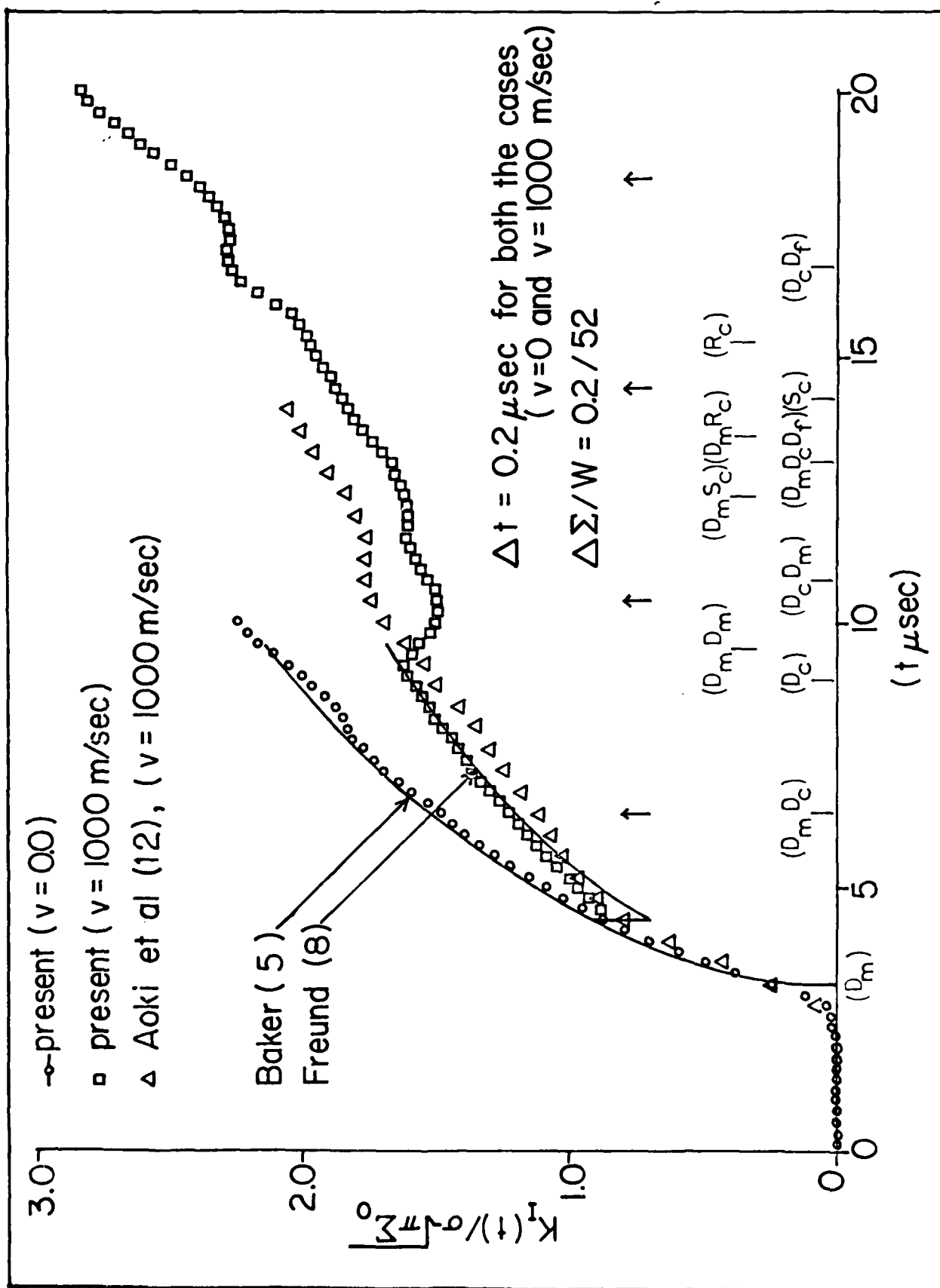


FIG. 7

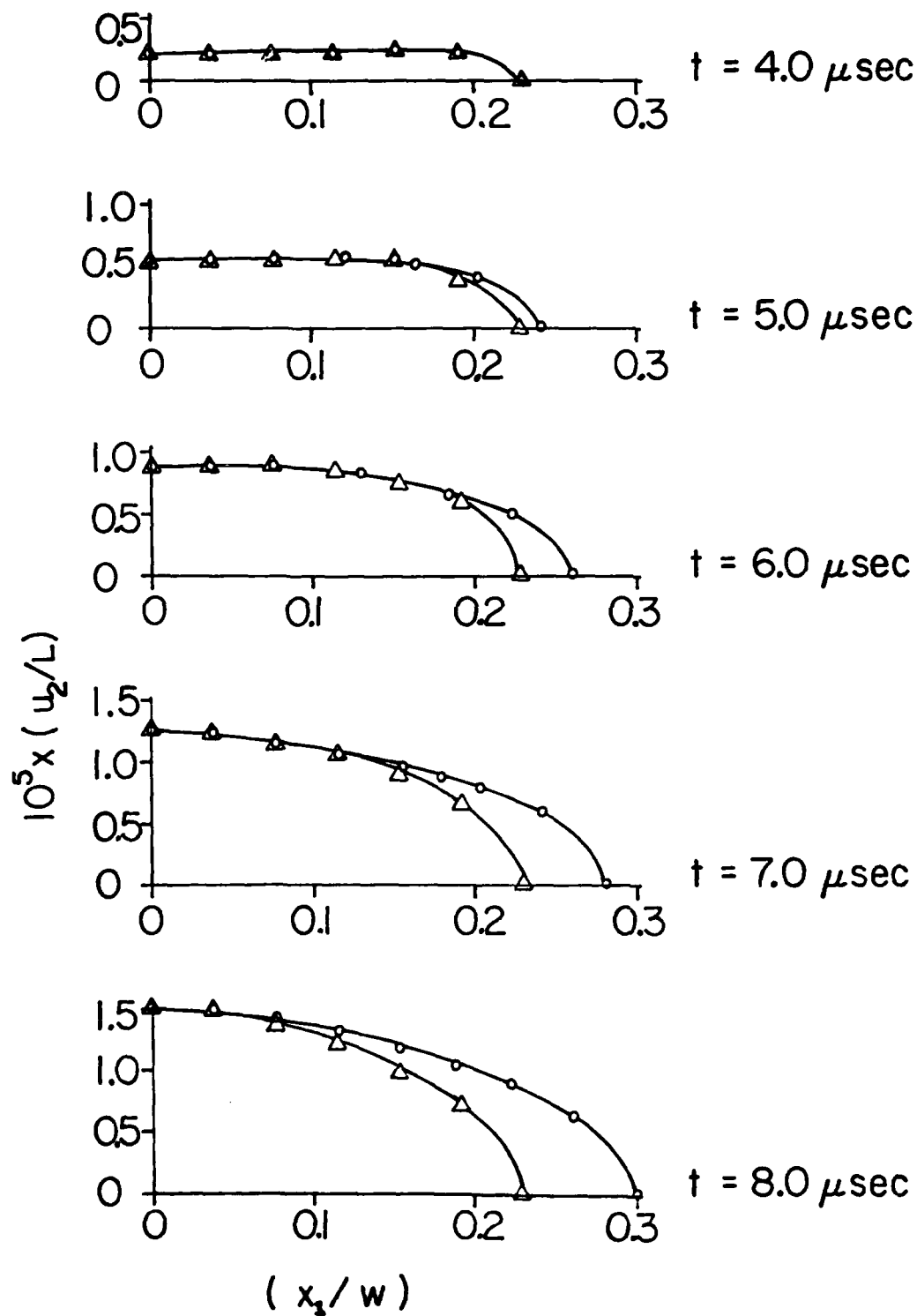
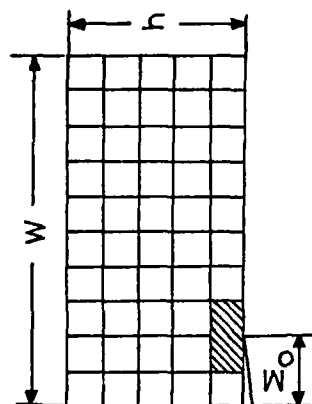


Fig. 8

$V = 0.2Cs$

- Present ($\Sigma_0/h = 0.4$, $W/h = 2.0$)
- Nilsson ($\Sigma_0/h = \infty$, $W/h = \infty$), [9]

$$K_S^\infty = \frac{\bar{U}_2 E}{h^{1/2} (1-\nu^2)}$$



$W = 40 \text{ mm}$

$h = 20 \text{ mm}$

$\Sigma_0 = 8 \text{ mm}$

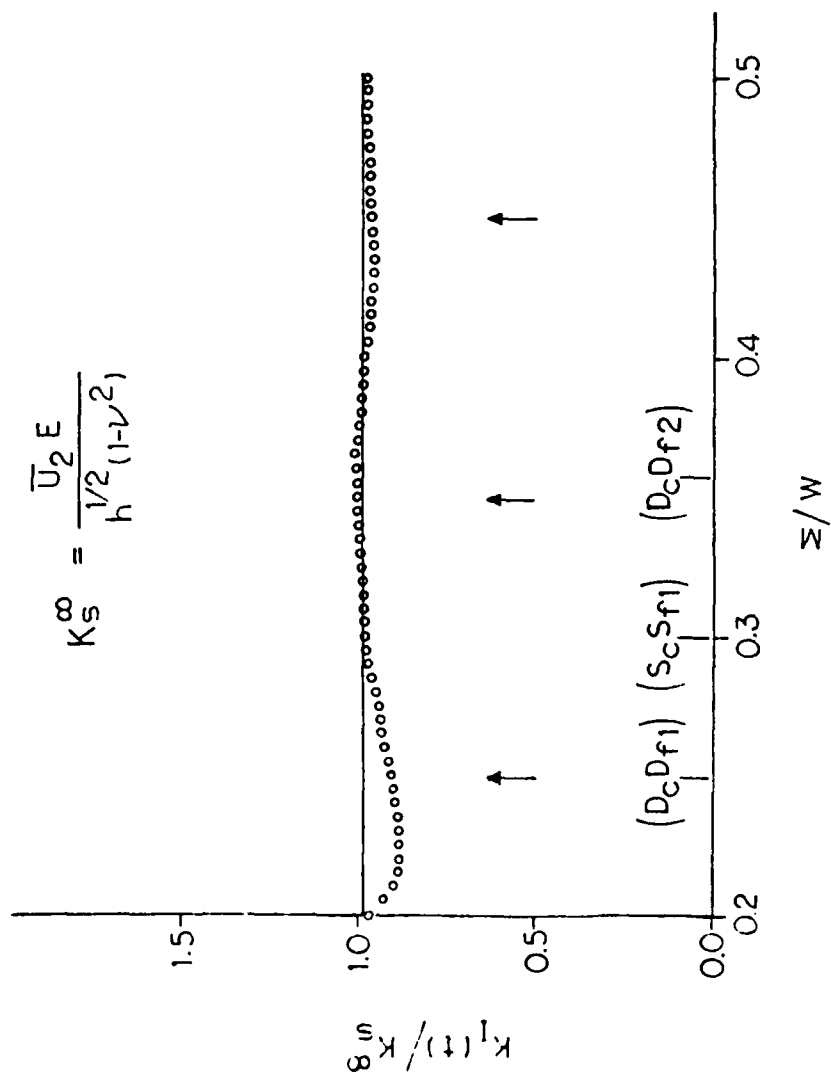


Fig. 9

$$V = 0.4 C_S$$

- Present ($\Sigma_0/h = 0.4$, $w/h = 2.0$)
- Nilsson ($\Sigma_0/h = \infty$, $w/h = \infty$), [9]

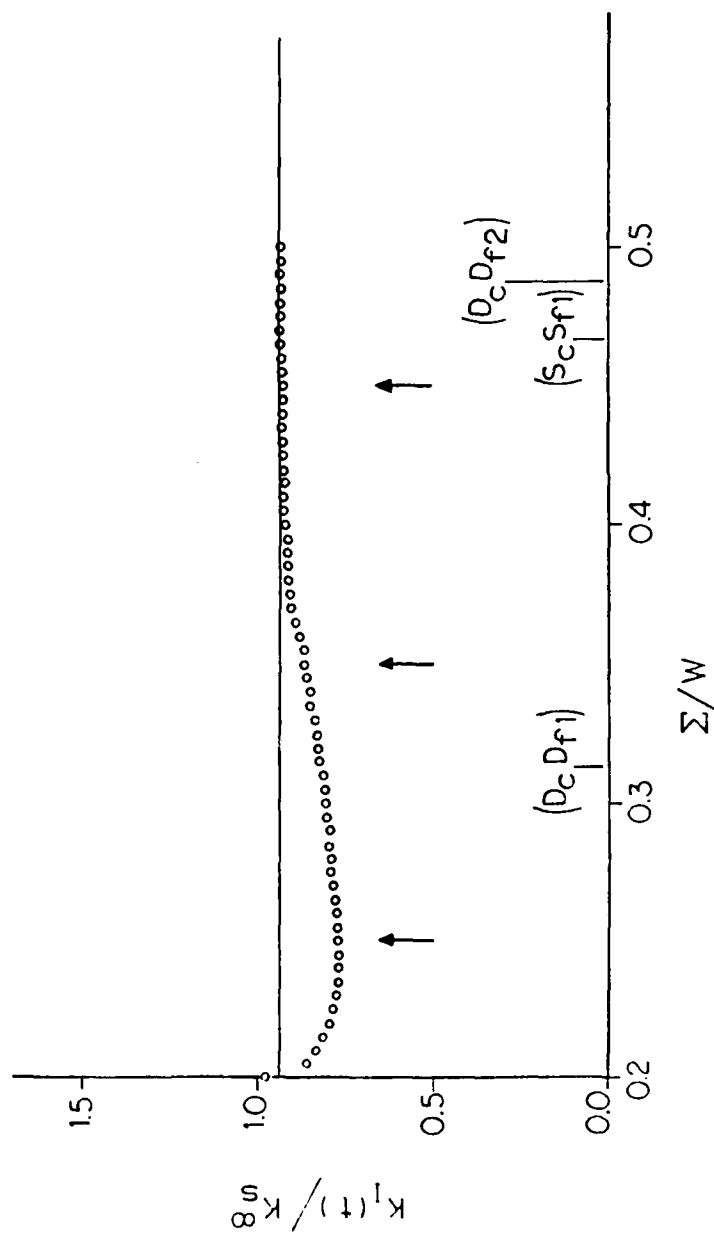


FIG. 10

$$V = 0.6 C_S$$

- Present ($\Sigma_0/h = 0.4, W/h = 2.0$)
- Nilsson ($\Sigma_0/h = \infty, W/h = \infty$)

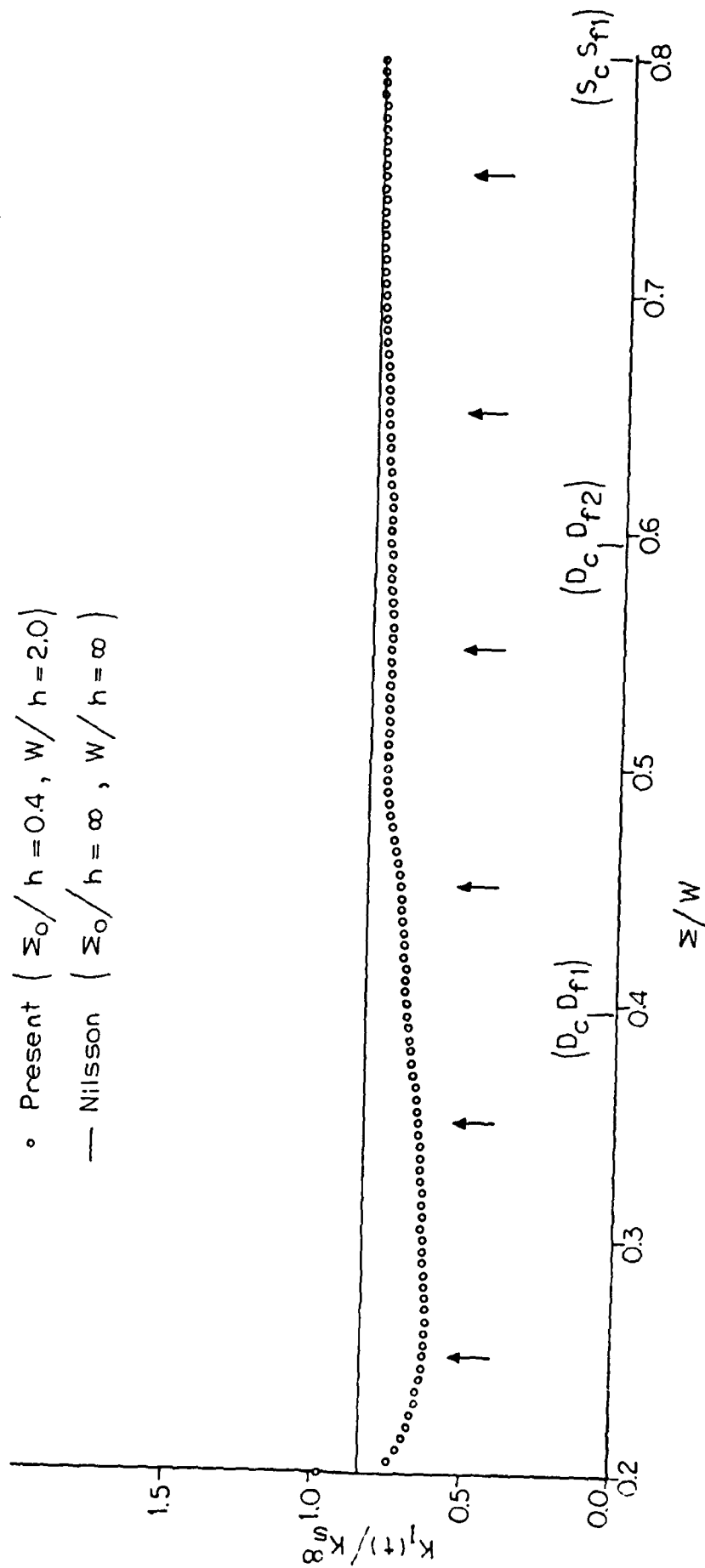


FIG. 11

Figure Captions

- Fig. 1 Calculation of Static K_I factors in a center-cracked tension specimen by the present "moving-singularity" method: $\Delta\Sigma = 0.005$. (+) indicates the current crack length when the regular element are readjusted as shown in Fig. 2 of [1].
- Fig. 2 Normalized Dynamic Stress intensity factor for a crack starting from a finite initial length and propagating with constant velocity, $v/C_s = 0.2$.
- Fig. 3 Normalized Dynamic Stress intensity factor, $(v/C_s) = 0.4$.
- Fig. 4 Normalized Dynamic Stress intensity factors for the cases $(v/C_s) = 0.6$ and 0.8 .
- Fig. 5 Crack-face Displacements at various time-instants, for a crack propagating at constant velocity, $(v/C_s) = 0.4$.
- Fig. 6 Time-Dependence of dynamic stress-intensity factor for a center-cracked rectangular plate subjected to Heaviside step-function normal stress.
- Fig. 7 Time-Dependence of dynamic stress-intensity factor for a center-cracked rectangular plate subject to a step-function normal stress. Crack remains stationary until t_0 and then propagates with a constant velocity.
- Fig. 8 Crack-face profiles for a stationary as well as propagating crack at various times.
- Fig. 9 Dynamic stress-intensity factor for an edge cracked square sheet subject to constant normal displacement: $(v/C_s) = 0.2$.
- Fig. 10 Dynamic stress-intensity factor for an edge cracked square sheet subject to constant normal displacement: $(v/C_s) = 0.4$.
- Fig. 11 Dynamic stress-intensity factor for an edge cracked square sheet subject to constant normal displacement: $(v/C_s) = 0.6$.

Accession For	
NTIS GRA&I	<input checked="checked" type="checkbox"/>
DDC TAB	<input type="checkbox"/>
Unannounced	<input type="checkbox"/>
Justification	<input type="checkbox"/>
By _____	
Distribution/ _____	
Availability Codes	
Dist	Avail and/or special
A	

REPORT DOCUMENTATION PAGE		READ INSTRUCTIONS BEFORE COMPLETING FORM
1. REPORT NUMBER GIT-CACM-SNA-25	2. GOVT ACCESSION NO. AD-A087228	3. RECIPIENT'S CATALOG NUMBER
4. TITLE (and Subtitle) Numerical Modeling of Dynamic Crack Propagation in Finite Bodies, by Moving Singular Elements - Part II. Results		5. TYPE OF REPORT & PERIOD COVERED Interim Report
7. AUTHOR(s) T. Nishioka, and S.N. Atluri		6. PERFORMING ORG. REPORT NUMBER GIT-CACM-SNA-25
9. PERFORMING ORGANIZATION NAME AND ADDRESS Center for the Advancement of Computational Mechanics School of Civil Engineering Georgia Institute of Technology, Atlanta, GA 30332		8. CONTRACT OR GRANT NUMBER(s) N00014-78-C-0636
11. CONTROLLING OFFICE NAME AND ADDRESS Office of Naval Research Structural Mechanics Program Dept. of the Navy, Arlington, VA 22217		10. PROGRAM ELEMENT, PROJECT, TASK AREA & WORK UNIT NUMBERS NR 064-610
14. MONITORING AGENCY NAME & ADDRESS (if different from Controlling Office)		12. REPORT DATE June 1980
		13. NUMBER OF PAGES 27
		15. SECURITY CLASS. (of this report) Unclassified
16. DISTRIBUTION STATEMENT (of this Report) Unlimited		15a. DECLASSIFICATION/DOWNGRADING SCHEDULE
<div style="border: 1px solid black; padding: 5px; text-align: center;"> <p>This document has been approved for public release and sale; its distribution is unlimited.</p> </div>		
17. DISTRIBUTION STATEMENT (of the abstract entered in Block 20, if different from Report)		
18. SUPPLEMENTARY NOTES to appear in <u>Jnl. of Appl. Mech.</u> Trans. ASME, 1980		
19. KEY WORDS (Continue on reverse side if necessary and identify by block number) Dynamic Fracture, Stress waves, Generation Study, Singular Finite Elements		
20. ABSTRACT (Continue on reverse side if necessary and identify by block number) Using the moving-singularity finite element method described in Part I of this paper, several problems of dynamic crack propagation in finite bodies have been analysed. Discussions of the effects of wave interactions on the dynamic stress-intensity factors are presented. The obtained numerical results are compared with the corresponding infinite domain solutions and other available numerical solutions for finite domains.		